

# The vacancy - edge dislocation interaction in fcc metals: a comparison between atomic simulations and elasticity theory

Emmanuel Clouet,

*Service de Recherches de Métallurgie Physique, CEA/Saclay,  
91191 Gif-sur-Yvette, France*

---

## Abstract

The interaction between vacancies and edge dislocations in face centered cubic metals (Al, Au, Cu, Ni) is studied at different length scales. Using empirical potentials and static relaxation, atomic simulations give us a precise description of this interaction, mostly in the case when the separation distance between both defects is small. At larger distances, elasticity theory can be used to predict this interaction. From the comparison between both approaches we obtain the minimal separation distance where elasticity applies and we estimate the degree of refinement required in the calculation. In this purpose, isotropic and anisotropic elasticity is used assuming a perfect or a dissociated edge dislocation and considering the size effect as well as the inhomogeneity interaction.

*Key words:* dislocation, vacancy, atomic simulations, elastic modeling

*PACS:* 61.72.Ji, 61.72.Yx

---

## 1 Introduction

Understanding the interaction between dislocations and vacancies is a key point in material science. In metal plasticity, this interaction controls dislocation climb and thus the plastic strain of a metal at high temperature when the glide of dislocations is blocked by obstacles like precipitates or the dislocation forest. This interaction also plays an important role in phase transformations. Indeed, as dislocations act as sinks and sources for vacancies, they control the way vacancies adjust their concentration in non-isothermal kinetics and thus

---

*Email address:* [emmanuel.clouet@cea.fr](mailto:emmanuel.clouet@cea.fr) (Emmanuel Clouet).

the diffusion. Moreover, the vacancy super-saturation along dislocations leads to an enhancement of diffusion in their vicinity: dislocations behave thus as short-circuits, a phenomenon known as pipe diffusion.

The interaction between vacancies and dislocations can be modeled using elasticity theory (for a review, see Ref. 1). In 1949, Cottrell and Bilby calculated the so-called size contribution, showing that the interaction energy is equal to the pressure created by the dislocation times the relaxation volume due to the vacancy [2]. This energy is thus decreasing with the inverse of the distance between both defects. In 1961, Bullough and Newman applied results of Eshelby theory [3,4] and brought out another contribution, the inhomogeneity interaction [5]. This contribution is proportional to the square of the pressure and of the shear stress created by the dislocation and is always attractive. It is much shorter range than the size contribution as it is decreasing with the square of the inverse of the distance. Such results are based on a continuum description of matter and assumes that a vacancy can be modeled by an inclusion having different elastic constants from the matrix.

First atomic calculations of the interaction between vacancies and dislocations [6–11] were used to check the validity of the elasticity theory and to obtain results in the vicinity of the dislocation core where a continuum description breaks down. For face centered cubic (fcc) metals [8,11], the vacancy binding energy was found to reach a maximum in the region of the stacking fault rather than in the immediate vicinity of the partial dislocations. More surprisingly, the vacancy was found to be attracted to a dissociated edge dislocation both above and below its glide plane. Some authors interpreted that as a manifestation of the inhomogeneity interaction [8]. In the same way, for body centered cubic metals, an anomalous positive binding energy was found in some cases on the tensile side of the dislocation elastic field [6,7] and the comparison with elastic models show discrepancies even for large separation distances [6,10]. Most of these simulations have been performed before the development in the mid-eighties of reliable empirical potentials for metals, like the embedded atom method (EAM) [12] or the tight-binding second-moment approximation (TB-SMA) [13,14]. They were based on pair potentials which fail to correctly predict elastic behavior. In particular, all cubic crystals modeled with pair potentials have to obey the Cauchy relation, which restricts the elastic constants  $C_{12}$  and  $C_{44}$  to be equal. Therefore, one can legitimately wonder whether results obtained with these potentials are not biased. On the other hand, EAM and TB-SMA potentials do not suffer such restrictions and have been shown to be well suited to study dislocation behavior. Some authors used these potentials to study the behavior of vacancies in the vicinity of dislocations, in particular to simulate pipe-diffusion in fcc metals [15–20]. These studies showed that the most stable position of the vacancy lies at the edge of the supplementary half plane corresponding to a partial dislocation and that diffusion is faster along dislocations than in the bulk. Nevertheless,

no careful comparison between atomic simulations and elasticity theory was performed. Such a comparison is useful to determine the range of validity of a continuum representation and the degree of refinement needed by elasticity. Indeed, not all materials properties can be modeled at the atomic scale and a description of the behavior of the material intrinsic defects at a larger scale is still needed. It is particularly true for plasticity where properties are linked to the collective behavior of dislocations which has to be modeled at a larger scale than the atomic one. It is thus interesting to see what conclusions can be drawn at the atomic scale with empirical potentials and how these results compare with predictions of the elasticity theory.

In the present work, we study the interaction between vacancies and dislocations in fcc metals at the atomic scale using EAM potentials and at a mesoscopic scale with the elasticity theory. We limit the discussion to edge dislocations as creep is controlled by their climb and thus by their interaction with vacancies when an external stress is applied. Several metals having the fcc structure are studied so as to bring out general results for fcc metals and identify a possible influence of the material properties, like the stacking fault energy or the elastic behavior. The results presented in this article are directly obtained from atomic simulations and then compared with predictions of the elasticity theory using different levels of approximation.

## 2 Atomic simulations

### 2.1 Interatomic potentials

The atomic simulations in this work are performed using empirical potentials of the EAM type. Such potentials are widely used to study dislocation properties as they present a good compromise between the size of the system which can be simulated and the realism of dislocation simulations. So as to test the generality of the results, various metals with the fcc structure are examined. The corresponding potentials are the ones developed by Ercolessi and Adams for Al [21], by Medlin et al. for Au [22], by Mishin et al. for Cu [23], and by Angelo et al. for Ni [24]. Some potentials leading to a better description of these metals properties may exist in the literature, but the purpose of this study is mainly to draw the main features of the vacancy-dislocation interaction which are common to fcc metals and to test the validity of the elastic theory compared to atomic simulations. In this purpose, the chosen EAM potentials appear to be well-suited as they cover a wide range of properties, as summarized in Tab. 1. For instance, Au potential leads to a low stacking fault energy  $\gamma$  and Al potential to a high one. Concerning their elastic behavior, Al potential appears to be almost isotropic ( $A \sim 1$ ) whereas Cu potential is

strongly anisotropic. Moreover, Al potential gives quite soft elastic constants whereas Ni potential gives hard ones. At last, the vacancy energy of formation obtained in Al is low compared to the one in Ni.

## 2.2 Simulation cell

The main characteristics of the unit cell used for atomic simulations are adapted from those used in [26–28] and are sketched in Fig. 1a. The  $x$ ,  $y$ , and  $z$  directions are parallel, respectively, to the  $[110]$ ,  $[1\bar{1}2]$ , and  $[\bar{1}11]$  directions. With such orientations, perfect edge dislocations can easily be introduced with a glide plane lying between two  $(\bar{1}11)$  planes, a line direction along the  $[1\bar{1}2]$  axis and a Burgers vector along the  $[110]$  axis. As periodic boundary conditions are used in all directions, two edge dislocations with opposite Burgers vectors have to be introduced in the simulation box. The distance between the two corresponding glide planes is chosen as half the height of the simulation box. According to elasticity theory, these two interacting dislocations form a

Table 1

Properties of the different EAM potentials: lattice parameters  $a$ , vacancy energy of formation  $E_V^f$ , vacancy relaxation volume  $\delta\Omega_V$ , stacking fault energy  $\gamma$ , elastic constants  $C_{11}$ ,  $C_{12}$ , and  $C_{44}$ , elastic anisotropy factor  $A$ , isotropic shear modulus  $\mu$  and Poisson coefficient  $\nu$  given by Voigt average (Eq. 3), and dissociation distance as given by isotropic ( $d^{\text{iso}}$ ) and anisotropic ( $d^{\text{ani}}$ ) elastic theories and atomic simulations ( $d^{\text{ato}}$ ).

Potential	Al [21]	Au [22]	Cu [23]	Ni [24, 25]
$a$ (Å)	4.032	4.079	3.615	3.52
$E_V^f$ (eV)	0.693	0.873	1.272	1.592
$\delta\Omega_V$ (Å <sup>3</sup> )	-6.6	-10.0	-3.5	-1.9
$\gamma$ (mJ.m <sup>-2</sup> )	104	30.7	44	89
$C_{11}$ (GPa)	118	185.8	170	246
$C_{12}$ (GPa)	62.3	157.1	123	147
$C_{44}$ (GPa)	36.7	38.9	76.2	125
$A = 2C_{44}/(C_{11} - C_{12})$	1.32	2.71	3.2	2.5
$\mu$ (GPa)	33.2	29.1	55.2	94.7
$\nu$	0.320	0.418	0.324	0.277
$d^{\text{iso}}$ (Å)	11.7	43.4	37.0	27.5
$d^{\text{ani}}$ (Å)	11.7	41.7	35.0	26.7
$d^{\text{ato}}$ (Å)	15	40	31	25

stable dipole for a  $\pi/4$  angle between the vector linking the centers of the dislocation lines and the glide planes [29]. This result holds for an isolated dipole, but, due to periodic boundary conditions, the dipole in the simulation box interacts with an infinity of dipoles. We thus choose to put a distance equal to the half of the unit cell dimension in the  $[110]$  direction and we find this position to be stable. One should notice that dislocations in the simulation box are straight dislocations and do not have any kink nor jog.

The atomic positions and the shape of the unit cell are relaxed at 0 K using a conjugate gradient algorithm. As expected, each edge dislocations dissociates into two partial dislocations separated by a stacking fault [29,30]. Atoms belonging to the core of these partial dislocations do not show fcc nor hexagonal compact neighborhood. They can therefore be easily identified in the simulation box (Fig. 1b), allowing the “measurement” of the dislocation separation distance  $d^{\text{ato}}$ . In agreement with the variations of the stacking fault energies  $\gamma$ , this separation distance is small for Al, big for Au and in-between for Cu and Ni (Tab. 1). The convergence of the dissociation distance  $d^{\text{ato}}$  with the dimensions of the unit cell has been checked and is found to be good for stackings of 160 and 60 planes respectively in  $[110]$  and  $[\bar{1}11]$  directions

### 2.3 Vacancy-dislocation interaction

Using the different EAM potentials, we calculate the vacancy-dislocation interaction energy for all possible positions of the vacancy in the simulation box

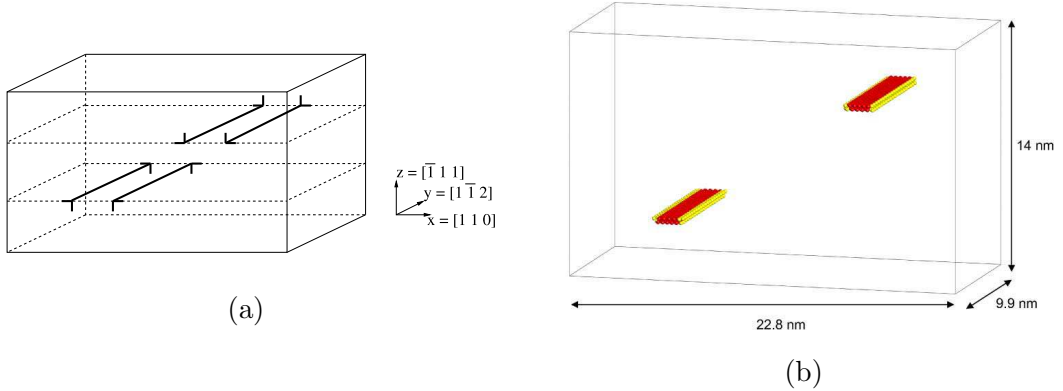


Fig. 1. (a) Sketch of the simulation cell showing the two dissociated edge dislocations and their glide plane. (b) Aluminum simulation box containing two edge dislocations. For clarity, only atoms belonging to the dislocations are shown: atoms in yellow (clear) are in the core of the partial dislocations and atoms in red (dark) in the stacking fault. The cell contains respectively 160, 120 and 60 in  $x$ ,  $y$  and  $z$  directions, corresponding to 190800 atoms.

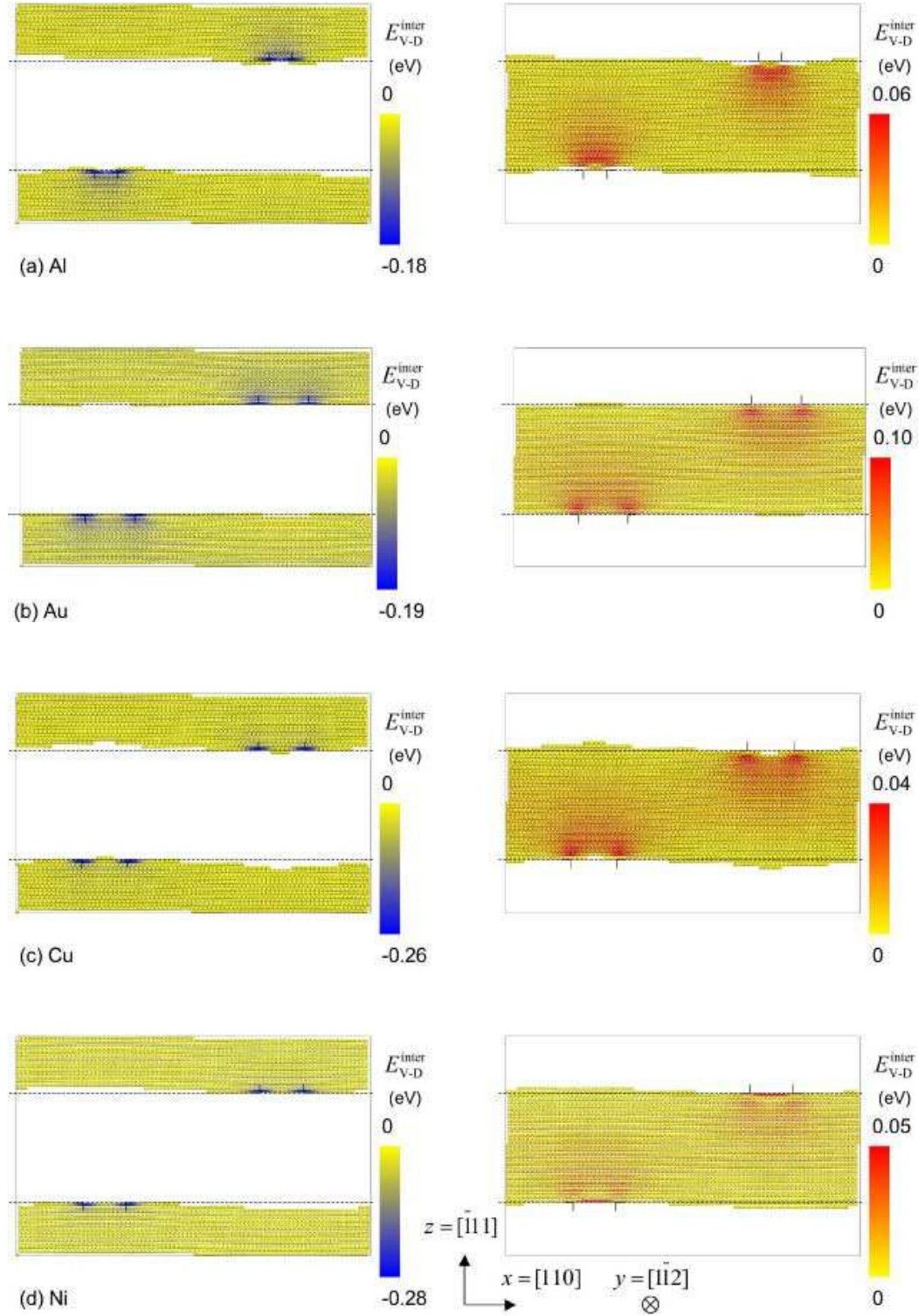


Fig. 2. Vacancy-dislocation interaction energy  $E_{V-D}^{\text{inter}}$  in (a) Al, (b) Au, (c) Cu, and (d) Ni as given by EAM potentials. On the left part of the figure, only attractive positions for the vacancy are shown ( $E_{V-D}^{\text{inter}} < 0$ ), whereas on the right part only repulsive positions are shown ( $E_{V-D}^{\text{inter}} > 0$ ). The positions of the partial dislocations and of their glide planes are sketched by lines.

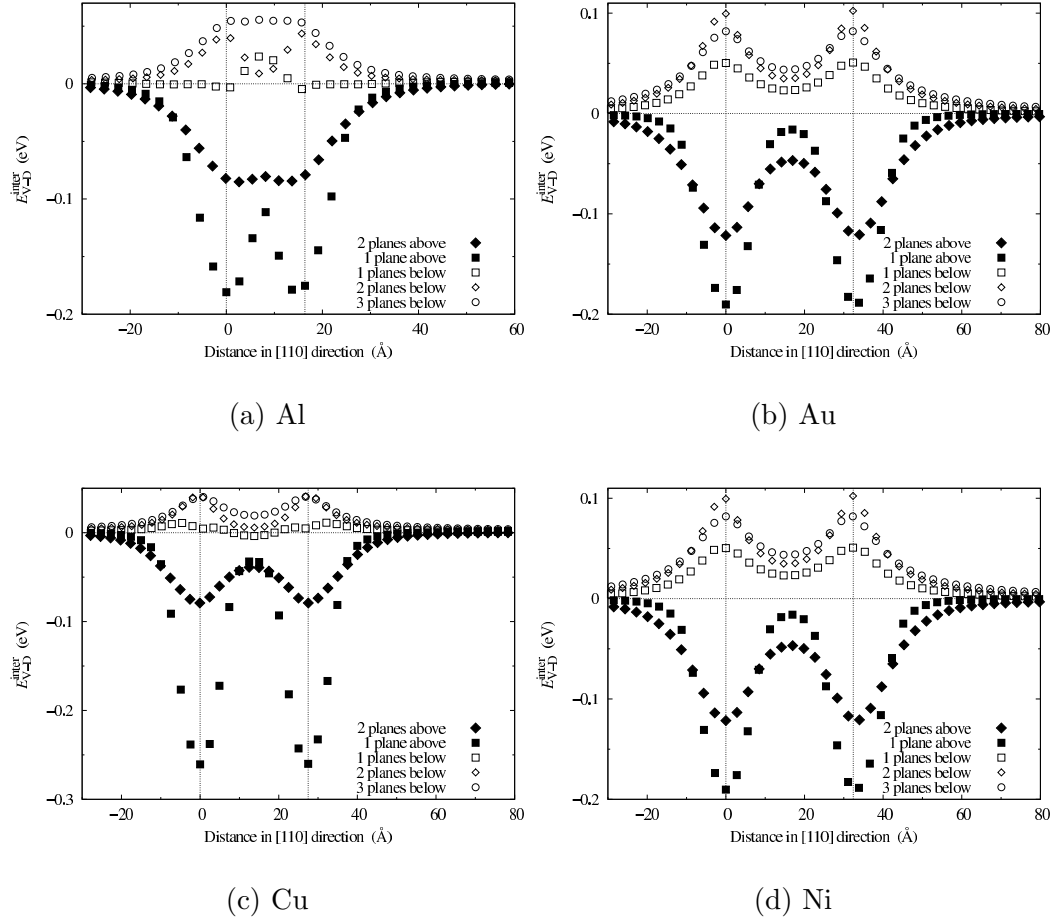


Fig. 3. Vacancy-dislocation interaction energy  $E_{V-D}^{\text{inter}}$  in (a) Al, (b) Au, (c) Cu, and (d) Ni as a function of distance from the center of one of the two partial dislocations. Scans are performed in the  $[110]$  direction for different  $(\bar{1}11)$  planes lying above (in the compressive zone) or below the glide plane (in the tensile zone). The origin is defined as the center of one of the two partial dislocations and axes are defined on Fig. 1a.

Table 2

Lowest vacancy-dislocation interaction energy  $E_{V-D}^{\text{inter}}$  (in eV) corresponding to a vacancy located on the edge of a partial dislocation.

Authors	Al	Au	Cu	Ni
Present work	-0.181	-0.190	-0.261	-0.279
Huang et al. [15]			-0.37	
Huang et al. [16]			-0.27	
Häkkinen et al. [17]			-0.14	
von Boehm et al. [18]		-0.11	-0.22	

with respect to the dislocations. This energy is defined as

$$E_{V-D}^{inter} = E + E_{V-D} - E_D - E_V, \quad (1)$$

where  $E$ ,  $E_{V-D}$ ,  $E_D$ , and  $E_V$  are the energy of the simulation box without any defect, with both the vacancy and the dislocations, with the dislocations only and with the vacancy only, respectively. All these energies are calculated after relaxing the atomic positions and the shape of the unit cell.

The calculations results are displayed both as functions of the vacancy positions (Fig. 2) and as energy profiles along lines parallel to the glide plane (Fig. 3). As expected, compressive regions attract the vacancy whereas tensile zones are repulsive. For potentials presenting a low stacking fault energy, an attractive and a repulsive basin can be associated with each one of the partial dislocations, as they are well dissociated. For Al it is not so clear since the separation distance between the two partial dislocations is smaller.

For all potentials, the most attractive position is located in the core of the partial dislocations, on the edge of the supplementary half-plane above the glide plane in the compressive region. This is in disagreement with first results obtained with pair potentials [8, 11] but confirms most recent studies using most reliable empirical potentials like EAM [17], TB-SMA [18], or pseudopotentials [15, 16]. The corresponding interaction energies are displayed in Tab. 2 and compared with previous calculations, showing a dependency on the potential used for a given metal. It seems that the higher the vacancy formation energy, the stronger the binding to the dislocation. Using the same potential for Al, Hoagland et al. [19] calculated the interaction energy of a vacancy with a screw dislocation ( $E_{V-D}^{inter} = -0.188$  eV) and Picu and Zang [31] with a  $60^\circ$  dislocation ( $E_{V-D}^{inter} = -0.163$  eV). The values obtained in these works are close to the one we find for an edge dislocation ( $E_{V-D}^{inter} = -0.181$  eV). Therefore, the binding of a vacancy to a dislocation seems to be quite independent on the dislocation character.

Looking at the variation of the interaction energy in the plane just above the glide plane in the compressive region (Fig. 3), one can see that the binding in the stacking fault is smaller than the one in the core of the partial dislocations. We do not observe a repulsion in the middle of the stacking fault as observed by Häkkinen et al. [17]. Thus a Suzuki segregation of vacancies is expected. Nevertheless, this large difference of the binding energies indicates that vacancies cannot easily migrate from one partial dislocation to the other as they have to cross the stacking fault. In such a case, one expects that diffusion is faster along the partial dislocation than in-between. This was shown by Fang and Wang [20] who used the same potential to calculate migration energies of a vacancy in Al. They obtained a higher energy for transverse core diffusion than for longitudinal core diffusion. Therefore, fast diffusion should occur along two well-separated pipes corresponding to the partial dislocations. Pipe

diffusion in a larger zone corresponding to the two pipes linked by a ribbon, as observed by Huang et al. [15, 16] in their molecular dynamic simulations, should only occur at high temperatures, where the partial dislocation cores spread over the stacking fault.

Above the glide plane, in the tensile zone, most of the vacancy positions are repulsive and only a few ones are slightly attractive. This contrasts with first atomic calculations which were performed with pair potentials and predicted an attraction of the vacancy above and below the glide plane [8, 11].

Concerning the configuration in which the repulsive interaction is maximum, one cannot draw a general situation. Indeed, for Au and Cu this position is located above the core of the partial dislocations, whereas for Al and Ni it is located in-between. Moreover, for Al and Cu, it lies three planes below the glide plane, for Au two planes below and for Ni only one plane below, i.e. in the habit plane of the stacking fault. We try to rationalize these differences by looking at the interaction energy  $E_{V-SF}^{\text{inter}}$  between the vacancy and the stacking fault (Fig. 4). When the vacancy lies in the habit plane of the stacking fault, this interaction is repulsive for Al and Ni, repulsive too for Au, but an order of magnitude lower, and attractive for Cu. This opposite interaction in the case of Cu arises from the fact that the stacking fault in Cu is in compression, whereas it is in tension in Al, Au and Ni. This was seen by computing the atomic pressure from the EAM potential using the definition of Vitek and Egami [32] (Fig. 4). This repulsive interaction with the stacking fault in Al and Ni adds, in the tensile zone, to the elastic repulsive interaction with the partial dislocations. Therefore the strongest repulsion is found between the partial dislocations. On the other hand, in the case of Cu, there is a compensation between the interactions with the stacking fault and the partial dislocations. Nevertheless, this explanation which tries to split the interaction in two different contributions does not really allow to predict the binding or the repulsion of the vacancy close to the dislocation. This shows

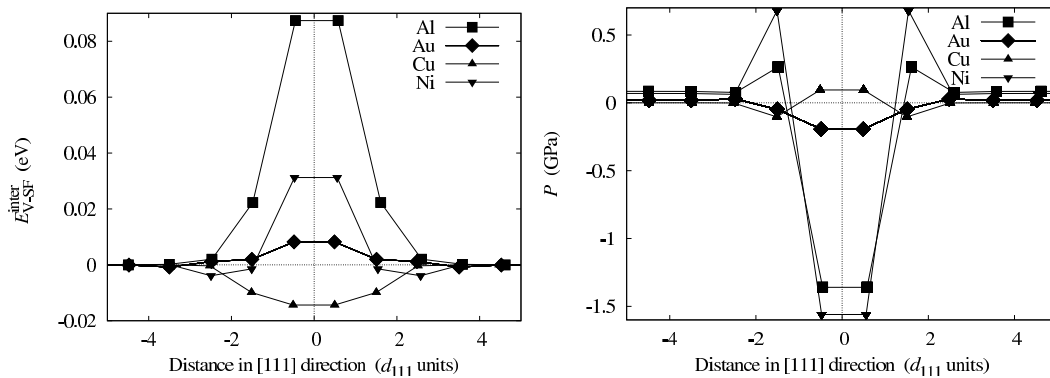


Fig. 4. Vacancy-stacking fault interaction energy  $E_{V-SF}^{\text{inter}}$  (left) and atomic pressure  $P$  (right) as functions of distance from the stacking fault. Distances are normalized by  $d_{111}$ , the interplanar distance in [111] direction in each material.

the usefulness of an atomic calculation close to the dislocation cores where the vacancy behavior is hard to predict.

### 3 Elasticity

As long as the vacancy is far enough from the dislocation, the interaction energy between both defects can be predicted using the elasticity theory. Considering only the first-order size interaction, this energy is simply given by [1, 2, 29, 30]

$$E_{V-D}^{\text{inter}} = P \delta\Omega_V, \quad (2)$$

where  $P = -(\sum_{ii} \sigma_{ii})/3$  is the pressure created by the dislocations at the lattice site where the vacancy lies and  $\delta\Omega_V$  is the vacancy relaxation volume. This last term is calculated directly from the atomic potential whereas the pressure is computed within the framework of the elasticity theory of dislocations [30]. Usually such calculations are performed assuming perfect dislocations and isotropic elasticity. However, dislocations are dissociated in fcc metals and not all materials can be assumed isotropic. We therefore check the validity of these different simplifying assumptions. For the isotropic elasticity calculations, we use the shear modulus  $\mu$ , the bulk modulus  $K$  and the Poisson coefficient  $\nu$ , obtained by Voigt average [30] of the elastic constants corresponding to the potential used for atomic calculations:

$$\mu = \frac{1}{5} (C_{11} - C_{12} + 3C_{44}), \quad (3a)$$

$$K = \frac{1}{3} (C_{11} + 2C_{12}), \quad (3b)$$

$$\nu = \frac{C_{11} + 4C_{12} - 2C_{44}}{2(C_{11} + 3C_{12} + C_{44})}. \quad (3c)$$

Whatever the assumptions used to calculate the pressure within the elasticity theory of dislocations, one has to cope with the problem of the periodic boundary conditions corresponding to the atomic simulations. Indeed, the two dislocations in the simulation box are not the only ones to consider in the elastic calculation. All their periodic images forming an infinite array of dipoles have to be included too. As the stress created by a dislocation is varying as the inverse of the distance, the sum associated with the calculation of the pressure is only conditionally convergent. To circumvent this numerical problem, we use the computational approach proposed by Cai<sup>1</sup> [33, 34].

---

<sup>1</sup> So as to compute the stress field created by this double periodic array of dislocations, one can take advantage too from the fact that each dislocation and its periodic images in the  $z$  direction form a tilt boundary. This causes a stress field which expression is analytical [30] and is known to decay exponentially with the

### 3.1 Perfect dislocations within the isotropic elasticity theory

Assuming isotropic elasticity, the pressure created by a perfect edge dislocation at a point of coordinates  $(x, y, z)$ <sup>2</sup> is

$$P_i = \delta_i \frac{\mu b}{3\pi} \frac{1 + \nu}{1 - \nu} \frac{z}{x^2 + z^2}, \quad (4)$$

where  $\delta_i = +1$  (conversely  $-1$ ) if the two supplementary half-plane corresponding to the edge dislocation  $i$  is in the  $z > 0$  (conversely  $z < 0$ ) sub-space and  $b = a\sqrt{2}/2$  is the Burgers vector of the perfect edge dislocation. This pressure, predicted by isotropic elasticity, can be used in Eq. 2 after summing pressures arising from all image dislocations so as to predict the interaction energy between the vacancy and the dislocations. In Fig. 5, we compare the elasticity theory predictions with values of  $E_{V-D}^{\text{inter}}$  previously calculated with EAM potentials, for different separation distances between both defects in the  $[110]$  and  $[\bar{1}11]$  directions. The elasticity theory manages to follow the atomic calculations as long as the vacancy is not too close to the dislocation core. For Al, a reasonable agreement is obtained for distances greater than  $\sim 10$  Å in  $[\bar{1}11]$  direction and greater than  $\sim 20$  Å in  $[110]$  direction. We believe that the elasticity theory is less accurate when the pressure is close to zero.

distance normal to the wall.

<sup>2</sup> The origin is defined as the center of the perfect dislocation and axes are defined on Fig. 1a.

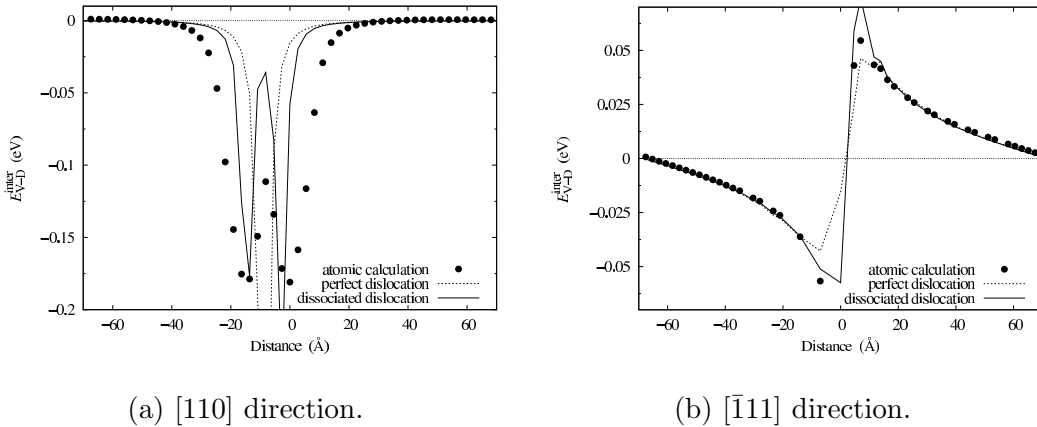


Fig. 5. Variation with the separation distance of the vacancy - dislocation interaction energy  $E_{V-D}^{\text{inter}}$  in  $[110]$  and  $[\bar{1}11]$  directions in Al. Symbols correspond to atomic simulation and lines to the isotropic elasticity theory (Eq. 2) assuming perfect or dissociated dislocations.

### 3.2 Influence of dislocations dissociation

We then examine whether considering the dissociation of the dislocations modifies the value of the interaction energy with the vacancy. According to isotropic elasticity theory, the dissociation distance is [29, 30]

$$d^{\text{iso}} = \frac{\mu b^2}{24\pi\gamma} \frac{2 + \nu}{1 - \nu}, \quad (5)$$

As presented in table 1, the dissociation distance predicted is quite close to the one observed in atomic simulations.

Only the edge components of each partial dislocations contribute to the pressure which becomes

$$P_i = \delta_i \frac{\mu b}{6\pi} \frac{1 + \nu}{1 - \nu} \left( \frac{z}{(x - d^{\text{iso}})^2 + z^2} + \frac{z}{(x + d^{\text{iso}})^2 + z^2} \right). \quad (6)$$

When the vacancy is close to the dislocation, the interaction energy  $E_{\text{V-D}}^{\text{inter}}$  calculated using the pressure, as given by Eq. 6, is in better agreement with atomic calculations than with the pressure given by Eq. 4. Even for Al, which has the smallest dissociation distance, the improvement is obvious (Fig. 5). When the separation distance between the vacancy and the dislocation becomes large compared to the dissociation distance ( $\sqrt{x^2 + z^2} \gg d^{\text{iso}}$ ), the difference between the dissociated and the non-dissociated cases becomes negligible since Eq. 6 converges to Eq. 4.

### 3.3 Influence of anisotropy

Instead of assuming isotropic elasticity to calculate the pressure created by a dislocation, one can use the elastic constants  $C_{11}$ ,  $C_{12}$  and  $C_{44}$  corresponding to the empirical potential of the atomic simulations and take full account of the anisotropy. Considering anisotropy can be quite significant in elastic calculations. For instance, two dilatation centers do not interact within isotropic elasticity, whereas there is an interaction when anisotropy is introduced. Moreover, Cai [33,34] showed that anisotropy has to be considered when calculating dislocation basic properties like their core energy or the Peierls stress.

Due to the symmetry in the  $[1\bar{1}2]$  direction along the dislocation line, finding the stress field associated with an edge dislocation is a two-dimensional problem and can be solved numerically following the sextic anisotropic elasticity theory of straight dislocations [30]. We thus calculate the elastic interaction between the two partial dislocations composing an edge dislocation so as to obtain its dissociation distance  $d^{\text{ani}}$ . The obtained value is really close to the

one calculated with isotropic elasticity (Tab. 1). The agreement with the distance observed in atomic simulation is slightly better but the difference is not really relevant, even for Cu which is the most anisotropic metal considered.

Using anisotropic elasticity theory to compute the pressure created by the dissociated edge dislocations, Eq. 2 gives another estimate for the interaction energy with vacancies. As shown for Cu in Fig. 6, the values of  $E_{V-D}^{\text{inter}}$  are similar to the ones calculated with isotropic elasticity. The agreement with atomic calculations is slightly better, but, as for the dissociation distance, the change due to anisotropy is negligible. Anisotropy does not lead to any significant change compared to isotropic calculations. Therefore, it does not need to be considered in the elastic calculation of the interaction energy of a vacancy with dislocations.

### 3.4 Inhomogeneity interaction

Another elastic interaction between the vacancy and the dislocation, the inhomogeneity contribution, needs to be considered [1, 5]. It arises from the fact that the vacancy has different elastic constants from the matrix. Thus, there is a change in the elastic energy that can be stored in the material. As the elastic constants that can be associated to the vacancy have to be lower than the ones of the matrix, this inhomogeneity interaction is always attractive. Indeed, the presence of a vacancy releases some elastic energy. Assuming that the elastic constants of the vacancy are null, one maximizes this contribution. In isotropic elasticity, the interaction energy between the vacancy and the

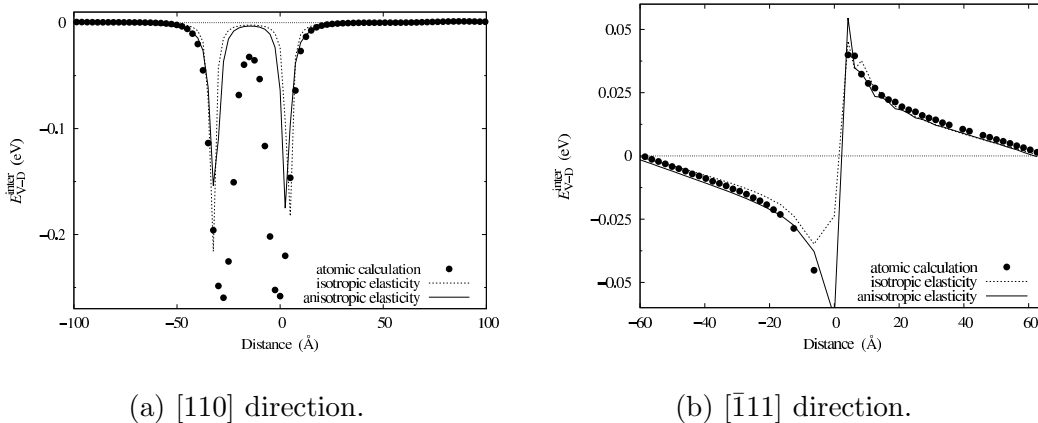


Fig. 6. Variation with the separation distance of the vacancy - dislocation interaction energy  $E_{V-D}^{\text{inter}}$  in [110] and  $[\bar{1}11]$  directions in Cu. Symbols correspond to atomic simulation and lines to the isotropic or anisotropic elasticity theory (Eq. 2) assuming dissociated dislocations.

dislocations now reads

$$E_{V-D}^{\text{inter}} = P \delta\Omega_V - \frac{1}{2}\Omega \left( \frac{3(1-\nu)}{2(1-2\nu)K} P^2 + \frac{5(1-\nu)}{(7-5\nu)\mu} \bar{\sigma}^2 \right), \quad (7)$$

where  $\bar{\sigma}$  is the Von-Misès equivalent stress and is related to the pure shear components of the stress created by the dislocation by

$$\bar{\sigma} = \sqrt{\frac{3}{2} \sum_{i,j} (\sigma_{ij} + P\delta_{ij})^2}. \quad (8)$$

Like the pressure, it can be easily computed for dissociated edge dislocations using isotropic elasticity. Considering the inhomogeneity contribution, the interaction energy now depends not only on the pressure but also on the shear stress. As it is varying linearly with the square of the stress, and thus with the square of the inverse of the distance between both defects, this contribution is much shorter range than the size contribution.

Considering the inhomogeneity contribution in the isotropic elasticity calculation of  $E_{V-D}^{\text{inter}}$  improves the agreement with atomic simulations close to the core of the partial dislocations, as can be seen for Ni in Fig. 7. In particular, without this contribution the interaction is symmetric with respect to the dislocation glide plane. The inhomogeneity interaction thus explains why the vacancy attraction in the compressive region is larger in magnitude than its repulsion in the tensile zone. This non-symmetric behavior of the interaction energy is clearly visible when the vacancy lies no more than one atomic distance from the dislocation core (Fig. 7(b)). For larger separation distances, the change induced by the inhomogeneity contribution is not significant. As

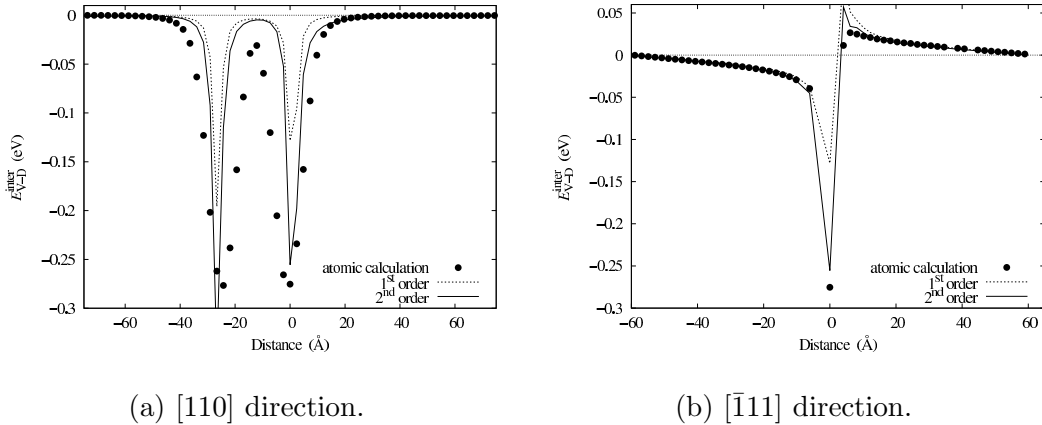


Fig. 7. Variation with the separation distance of the vacancy - dislocation interaction energy  $E_{V-D}^{\text{inter}}$  in [110] and  $[\bar{1}11]$  directions in Ni. Symbols correspond to atomic simulation and lines to the isotropic elasticity theory assuming dissociated dislocations. The first order approximation corresponds to Eq. 2 and the second order to Eq. 7.

pointed by Bullough and Newman [1], when this inhomogeneity interaction is taken into account in the elastic calculation, one should incorporate also the second-order size interaction arising from the non-linear elastic properties of the crystal, as both contributions are decreasing in the same manner with the distance. Eventhough this last term may lead to a better agreement with atomic calculations in the vicinity of the dislocation cores, we do not consider it since results based on non-linear elastic calculations are too complicated to handle. Therefore, we prefer to use only the linear elasticity theory, considering the fact that one can switch to atomic calculations for short separation distances where the theory breaks down.

## 4 Conclusions

The interaction between vacancies and edge dislocations has been modeled in fcc metals at different scales. When only a few atomic distances lie between the vacancy and the cores of the partial dislocations or the stacking fault an atomic description of this interaction is needed. Using empirical potentials, one finds for fcc metals that the most attractive position of the vacancy lies at the edges of the supplementary half-planes corresponding to the partial dislocations. Positions above the slip planes, in the compressive region, are always attractive whereas, below the slip planes, positions are repulsive or, for some metals like Cu and Ni, slightly attractive in the habit plane of the stacking fault.

When the separation distance between both defects is greater, the elasticity theory manages to predict quantitatively the interaction energy. One does not need to take into account anisotropy in the calculations as this does not lead to any significant change compared to an isotropic calculation. On the other hand, better agreement with atomic simulations is obtained for short separation distances, when the dislocation dissociation is considered. Taking into account the inhomogeneity interaction and not only the size effects improves predictions of the elastic calculation too. The most significant change is that the interaction energy is not anymore symmetric with respect to the dislocation glide plane.

## Acknowledgements

The author is grateful to Dr. A. Barbu, Dr. J.-L. Bocquet, Dr. M. Guttman, Dr. B. Legrand, Dr. D. Mordehai, and Prof. J.-P. Poirier for fruitful discussions.

## References

- [1] R. Bullough, R. C. Newman, The kinetics of migration of point defects to dislocations, *Rep. Prog. Phys.* 33 (1970) 101–148.
- [2] A. H. Cottrell, B. A. Bilby, Distribution of solute atoms around a slow dislocation, *Proc. Phys. Soc. London Ser. A* 62 (1949) 49.
- [3] J. D. Eshelby, The determination of the elastic field of an ellipsoidal inclusion, and related problems, *Proc. R. Soc. Lond.* A241 (1957) 376–396.
- [4] J. D. Eshelby, Elastic inclusion and inhomogeneities, in: I. N. Sneddon, R. Hill (Eds.), *Progress in Solid Mechanics*, Vol. 2, North Holland, 1961, pp. 87–140.
- [5] R. Bullough, R. C. Newman, The interaction of vacancies with dislocations, *Phil. Mag.* 7 (1963) 529–531.
- [6] R. Bullough, R. C. Perrin, Atomic configuration and nonlinear aspects of the core of dislocation in iron, in: A. R. Rosenfield, G. T. Hahn, A. L. Bement, R. I. Jaffee (Eds.), *Dislocation Dynamics*, McGraw-Hill Book Co., New York, 1968, pp. 175–190.
- [7] K. W. Ingle, A. G. Crocker, The interaction between vacancies and the  $\frac{1}{2} < 111 > (1\bar{1}0)$  edge dislocation in body centred cubic metals, *Acta Metall.* 26 (1970) 1461–1649.
- [8] R. C. Perrin, A. Englert, R. Bullough, Extended defects in copper and their interactions with point defects, in: P. C. Gehlen, J. R. Beeler, R. I. Jaffee (Eds.), *Interatomic Potentials and Simulation of Lattice Defects*, Plenum press, New York, 1972, pp. 509–524.
- [9] K. M. Miller, K. W. Ingle, A. G. Crocker, A computer simulation study of pipe diffusion in body centred cubic metals, *Acta Metall.* 29 (1981) 1599–1606.
- [10] R. H. J. Fastenau, M. I. Baskes, A combined atomistic and Monte Carlo simulation of point defect-dislocation interactions, *Phys. Stat. Sol. A* 75 (1983) 323–334.
- [11] L. I. Yakovenkova, L. Y. Kar’kina, G. L. Podchinenova, Structure of core of a dissociated dislocation and interaction energy with vacancies in f.c.c. crystals with different stacking fault energies, *Phys. Met. Metall.* 59 (1985) 48–53.
- [12] M. S. Daw, M. I. Baskes, Embedded-atom method: Derivation and application to impurities, surfaces, and other defects in metals, *Phys. Rev. B* 29 (1984) 6443–6453.
- [13] M. W. Finnis, J. E. Sinclair, A simple empirical N-body potential for transition metals, *Phil. Mag. A* 50 (1984) 45–56.
- [14] V. Rosato, M. Guillopé, B. Legrand, Thermodynamical and structural properties of fcc transition metals using a simple tight-binding model, *Phil. Mag. A* 59 (1989) 321–336.

- [15] J. Huang, M. Meyer, V. Pontikis, Is pipe diffusion in metals vacancy controlled? a molecular dynamics study of an edge dislocation in copper, *Phys. Rev. Lett.* 63 (1989) 628–631.
- [16] J. Huang, M. Meyer, V. Pontikis, Migration of point defects along a dissociated edge dislocation in copper: a molecular dynamics study of pipe diffusion, *Phil. Mag. A* 63 (1991) 1149–1165.
- [17] H. Häkkinen, S. Mäkinen, M. Manninen, Edge dislocations in fcc metals: Microscopic calculations of core structure and positron states in Al and Cu, *Phys. Rev. B* 41 (1990) 12441–12453.
- [18] J. von Boehm, R. M. Nieminen, Molecular-dynamics study of partial edge dislocations in copper and gold: Interactions, structures, and self-diffusion, *Phys. Rev. B* 53 (1996) 8956–8966.
- [19] R. G. Hoagland, A. F. Voter, S. M. Foiles, Self-diffusion within the cores of a dissociated glide dislocation in an fcc solid, *Scripta Mater.* 39 (1998) 598–596.
- [20] Q. F. Fang, R. Wang, Atomistic simulation of the atomic structure and diffusion within the core region of an edge dislocation in aluminum, *Phys. Rev. B* 62 (2000) 9317–9324.
- [21] F. Ercolessi, J. B. Adams, Interatomic potentials from first-principles calculations: the force-matching method, *Europhys. Lett.* 26 (1994) 583–588.  
URL <http://www.fisica.uniud.it/~ercolessi/potentials/Al/>
- [22] D. L. Medlin, S. M. Foiles, D. Cohen, A dislocation-based description of grain boundary dissociation: Application to a 90°  $\langle 110 \rangle$  tilt boundary in gold, *Acta Mater.* 49 (2001) 3689–3697.
- [23] Y. Mishin, M. J. Mehl, D. A. Papaconstantopoulos, A. F. Voter, J. D. Kress, Structural stability and lattice defects in copper: Ab initio, tight-binding, and embedded-atom calculations, *Phys. Rev. B* 63 (2001) 224106.
- [24] J. E. Angelo, N. R. Moody, M. I. Baskes, Trapping of hydrogen to lattice defects in nickel, *Modelling Simul. Mater. Sci. Eng.* 3 (1995) 289–307.
- [25] M. I. Baskes, X. Sha, J. E. Angelo, N. R. Moody, Trapping of hydrogen to lattice defects in nickel, *Modelling Simul. Mater. Sci. Eng.* 5 (1997) 651–652.
- [26] D. Rodney, G. Martin, Dislocation pinning by small interstitial loops: A molecular dynamics study, *Phys. Rev. Lett.* 82 (1999) 3272–3375.
- [27] D. Rodney, G. Martin, Dislocation pinning by glissile interstitial loops in a nickel crystal: A molecular-dynamics study, *Phys. Rev. B* 61 (2000) 8714–8725.
- [28] E. Rodary, D. Rodney, L. Proville, Y. Bréchet, G. Martin, Dislocation glide in model Ni(Al) solid solutions by molecular dynamics, *Phys. Rev. B* 70 (2004) 054111.
- [29] J. Friedel, *Dislocations*, Pergamon Press, Oxford, 1964.

- [30] J. P. Hirth, J. Lothe, Theory of Dislocations, 2nd Edition, Wiley, New York, 1982.
- [31] R. Picu, D. Zhang, Atomistic study of pipe diffusion in Al-Mg alloys, *Acta Mater.* 52 (2004) 161–171.
- [32] V. Vitek, T. Egami, Atomic level stresses in solids and liquids, *Phys. Status Solidi B* 144 (1987) 145–156.
- [33] W. Cai, Modeling dislocations using a periodic cell, in: S. Yip (Ed.), *Handbook of Materials Modeling*, Springer, The Netherlands, 2005, pp. 813–826.
- [34] W. Cai, V. Bulatov, J. Chang, J. Li, S. Yip, Periodic image effects in dislocation modelling, *Phil. Mag.* 83 (2003) 539–567.